research articles Journal of proteome research

Turnover of the Human Proteome: Determination of Protein Intracellular Stability by Dynamic SILAC

Mary K. Doherty,[‡] Dean E. Hammond,[‡] Michael J. Clague,[‡] Simon J. Gaskell,[§] and Robert J. Beynon*,[†]

Proteomics and Functional Genomics Research Group, Department of Veterinary Preclinical Sciences, University of Liverpool, Crown Street, Liverpool L69 7ZJ, United Kingdon, The Physiological Laboratory, School of Biomedical Sciences, University of Liverpool, Crown Street, Liverpool L69 3BX, United Kingdom, and Michael Barber Centre for Mass Spectrometry, Manchester Interdisciplinary Biocentre, University of Manchester, Princess Street, Manchester M1 7DN, United Kingdom

Received August 14, 2008

The proteome of any system is a dynamic entity, such that the intracellular concentration of a protein is dictated by the relative rates of synthesis and degradation. In this work, we have analyzed time-dependent changes in the incorporation of a stable amino acid resolved precursor, a protocol we refer to as "dynamic SILAC", using 1-D gel separation followed by in-gel digestion and LC-MS/MS analyses to profile the intracellular stability of almost 600 proteins from human A549 adenocarcinoma cells, requiring multiple measures of the extent of labeling with stable isotope labeled amino acids in a classic label-chase experiment. As turnover rates are acquired, a profile can be built up that allows exploration of the 'dynamic proteome' and of putative features that predispose a protein to a high or a low rate of turnover. Moreover, measurement of the turnover rate of individual components of supramolecular complexes provides a unique insight in processes of protein complex assembly and turnover.

Keywords: Protein turnover • mass spectrometry • dynamic SILAC

Introduction

The ability of a cell to replenish and adjust the constituent protein pool is a vital component of the modulation of response, but the continuous turnover of proteins in the cell is also a feature of an unstressed steady-state condition. Even when a cell is not undergoing a period of growth, the protein pool is dynamic, and considerable energy is expended in the continuous synthesis and degradation of most cellular proteins.[1,2] Different proteins turn over at distinctly different rates, ranging from seconds to months.[3] Proteins with a high turnover rate can be regulated by manipulation of the amount of protein in the cell, while low turnover proteins are either nonregulatory or are regulated through post-translational processes such as phosphorylation.

Many early studies of protein turnover were reliant on low level of incorporation of radiolabeled amino acids, and could only be expressed in terms of total protein dynamics.[4−7] In some cell systems, it was possible to monitor the degradation of individual proteins by [^{35}S] radiolabeling[8] and pulse-chase experiments,[9−11] often in experimental designs in which the reincorporation of label was eliminated by protein synthesis inhibitors such as cycloheximide, although there was residual concern that the use of such inhibitors disrupted normal degradative processes. Proteomic technologies have introduced the possibility of determining the turnover rates of multiple proteins simultaneously.[1,12−15] The ability to analyze vanishingly small amounts of protein, or peptides derived therefrom by mass spectrometry, and the ability to discriminate by mass a peptide labeled with a stable isotope tagged amino acid from the unlabeled peptide meant that, for the first time, it was possible to determine intracellular protein replacement rates (turnover) on a large scale. This not only allows rapid acquisition of data sets of protein stability, but also the integration of proteome dynamic data with that of transcriptome and metabolome data in a systems manner which will ultimately lead to a holistic, integrated understanding of cellular physiology.

Stable isotope labeling of cells in culture with amino acids (SILAC) in conjunction with mass spectrometry has facilitated relative quantification of proteins and post-translational modification (PTM) of proteins on a proteome-wide scale, but it is also applicable to the measurement of protein turnover. An early application of proteomics to analysis of protein turnover on a protein by protein basis was performed in *Saccharomyces cerevisiae*[15] and this technology has also been applied to *Escherichia coli*,[13] HeLa cell nucleoli,[12] *Mycobacterium smegmatis*,[16] human atrial trabeculae[17] and the chicken.[14] In the majority of cases, a stable isotope labeled amino acid is administered either via the cell medium or, for intact animals, with the diet. The protein fraction of interest is isolated from samples collected through the time-course of the experiment

* To whom correspondence should be addressed. E-mail: r.beynon@liverpool.ac.uk.
[‡] School of Biomedical Sciences, University of Liverpool.
[§] University of Manchester.
[†] Department of Veterinary Preclinical Sciences, University of Liverpool.

10.1021/pr800641v CCC: $40.75

Published on Web 10/28/2008

and simplified (1DGE, 2DGE, liquid chromatography). The simplified analyte is then subjected to mass spectrometric analysis.

Although the gross mechanisms through which protein turnover is achieved are relatively well understood, the intracellular signals that dictate which protein is to be degraded are not. A range of biochemical and biophysical properties of proteins have been highlighted as possible determinants of degradative rate. These include molecular weight,[18] isoelectric point,[19,20] hydrophobicity[21] and sequence motifs.[22,23] A recent study[24,25] indicated that the degree of disorder in a protein was a weak but dominant determinant of protein stability. For subsets of proteins, there is evidence for motifs (or degrons) that predispose a protein to a higher rate of turnover, including PEST sequences.[23] One degron that has aroused considerable interest is the N-degron, which most simply put, states that the N-terminal amino acid of a mature protein is the determinant of the rate of degradation.[22,26] This behavior, embodied as the N-end rule, has been extended and modified to include definitions of stabilizing residues, primary destabilizing residues and secondary destabilizing residues that must be conjugated to an arginine residue, through the action of arginine R-transferases. Finally, tertiary destabilizing residues are processed by N-terminal amidases to their corresponding acid form prior to arginine conjugation. The N-terminal amino acid is thought to be recognized by specific protein (N-recognins) that then direct the assembly of polyubiquitin chains on a lysine residue elsewhere in the protein sequence, hence, initiating the degradative process via the ubiquitin-proteasome system.[27,28]

In this study, the rates of degradation of almost 600 proteins from human A549 lung adenocarcinoma cells have been determined. This has allowed a comprehensive examination of the numerous parameters that have been linked to individual protein degradation rate and presents a targeted interrogation of the determinants believed to dictate inherent protein intracellular stability.

Experimental Procedures

Cell Culture Media Preparation and Cell Culture Conditions. The cell culture medium, Dulbecco's Modified Eagles Medium (DMEM) modified to be deficient in arginine, lysine and leucine, was a custom preparation from Invitrogen (Paisley, U.K.). [$^{13}C_6$] L-Arginine (98% purity) was obtained from Cambridge Isotope Laboratories (Andover, MA). All other L-amino acids were obtained from Sigma (Gillingham, U.K.). Foetal bovine serum (FBS) was obtained from Invitrogen and dialysed twice for 24 h against a 10-fold volume excess of phosphate buffered saline (PBS). The appropriate amount of amino acids was added to the amino-acid deficient medium according to the manufacturer's specifications for standard DMEM, with the exception of arginine. The arginine-free medium was then divided in two lots and 28 mg/L of either L-Arginine or [$^{13}C_6$] L-Arginine added separately to make up the Arg-0 (light-Arg) or Arg-6 (heavy-Arg) media, respectively. Each medium was supplemented with 2 mM L-glutamine (Sigma) and 10% dialysed FBS and then sterile-filtered through a 0.22 μm filter (Corning, Schiphol-Rijk, The Netherlands). Human adenocarcinoma A549 cells were cultured in heavy-Arg (Arg-6) DMEM-labeling media for 13 days. The labeled medium was removed and the cells were quickly washed twice with sterile PBS at 37 °C. The cells were then incubated with unlabeled light-Arg (Arg-0) DMEM media for "chase" periods of 0, 0.25, 0.5, 1, 2, 4 or 8 h after which the cells were washed on ice with ice-cold PBS, then scraped off the dishes, pelleted by centrifugation and snap-frozen in liquid nitrogen. The pelleted cells from two replicates were pooled and stored at −80 °C.

Gel Electrophoresis. Cell pellets were resuspended in deionized water containing protease inhibitors (Complete Protease Inhibitors, Roche, Lewes, U.K.) and the cells lysed by sonication with the supernatant fraction being retained for analysis. The protein content of each sample was assayed using the Coomassie Plus Protein Assay (Perbio Science UK Ltd., Tattenhall, U.K.). Proteins (10 μg per lane) were separated by electrophoresis through a 12.5% (w/v) SDS-PAGE gel and stained with Coomassie blue. All samples were analyzed simultaneously. Each gel lane was divided into 40 equal slices and the proteins were subjected to in-gel tryptic digestion and peptide extraction using a MassPrep digestion robot (Waters Micromass, Manchester, U.K.) using previously published protocols.[29]

Mass Spectrometric Analysis. Peptides were resolved over a 50 min 0−80% (v/v) acetonitrile gradient by nanospray reversed phase chromatography (Dionex Ultimate 3000, C18 Pepmap (5 mm × 300 μm i.d.) precolumn, coupled with a C18 Pepmap (15 cm × 75 μm i.d.) column) prior to mass spectrometry (Thermo Electron LTQ). Peptides were analyzed using "triple-play" data-dependent acquisition. For each full mass range scan, the zoom scan (mass window = 10 Da) and subsequent MS/MS spectrum were obtained sequentially for three peptide ions in a single cycle. Dynamic exclusion parameters were set to minimize the repeat acquisition of intense ions. Raw spectra were converted to .mgf files using DTAsupercharge[30] prior to database searching with a locally implemented MASCOT server. The initial search parameters allowed for a single trypsin missed cleavage, carbamidomethyl modification of cysteine residues, oxidation of methionine, a peptide mass tolerance of ±1.5 Da and a fragment mass tolerance of ±0.8 Da. Peptide charge was +1, +2, +3 and the data was searched against MSDB, taxonomy, *Homo sapiens*. An additional parameter, coded as a pseudo post-translational modification was included to search (automatically or manually) for peptides containing [$^{13}C_6$]-arginine. The software package MSQuant[30] was used to identify and quantify peptides that contained stable isotope labeled arginine at different time points during the unlabeled 'chase' experiment. From these data, the loss of labeled peptide was analyzed by nonlinear curve fitting to derive the rate of loss of label from the protein pool, and subsequently corrected by protein pool dilution due to cell growth to yield the first order rate constant for degradation of the protein.

Functional Analysis. To assign a functional category to each of the proteins, the Human Protein Reference Database Web site (http://www.hprd.org/) was used. This classifies proteins according to cellular location, class, function and biological process. SignalP (http://www.cbs.dtu.dk/services/SignalP/) was used to determine whether any of the proteins had N-terminal signal peptides. Any signal peptides were removed prior to the determination of molecular weight, p*I* or N-terminal residue. Molecular weight and p*I* of the mature proteins were determined using the ProtParam tool (www.expasy.org). N-Terminal residue was determined by manual inspection of each protein sequence. The extent of disorder was calculated using the FoldIndex program.[31]

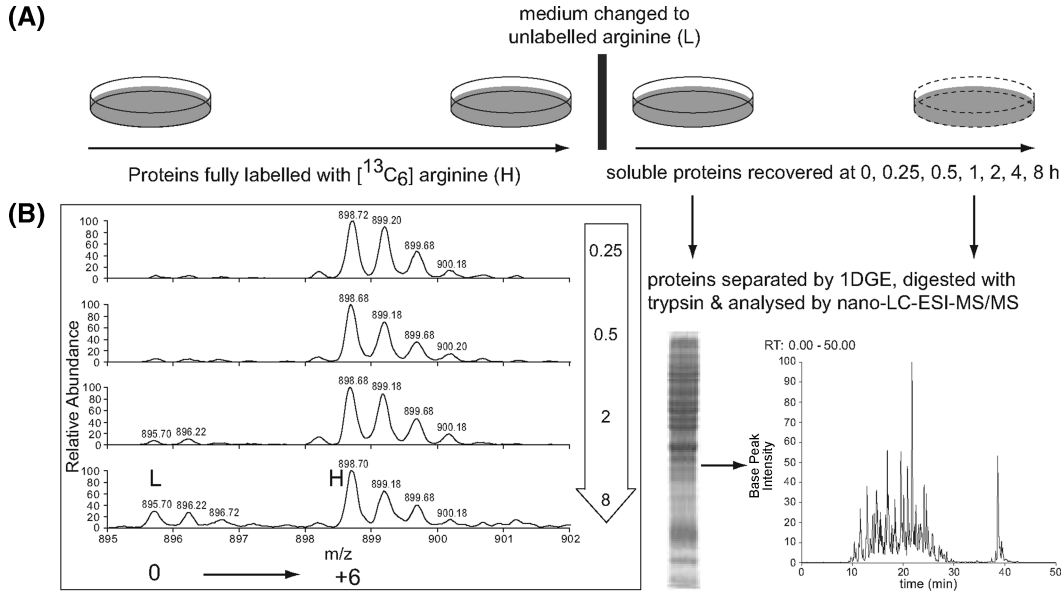

Figure 1. Strategy for protein turnover measurements. (A) Cells were grown in media supplemented with [$^{13}C_6$]-arginine and subsequently "chased" by transfer to a medium containing unlabeled arginine. Proteins from each time point were separated by SDS-PAGE and each lane was divided into 40 slices. A representative total ion chromatogram (base peak) from one slice after tryptic digestion and LC-MS/MS analysis is shown. (B) The relative incorporation of the heavy and light amino acid into multiple proteins was determined over an 8 h period, from which the first order rate constant for replacement of the protein was determined by nonlinear curve fitting.

Results and Discussion

Following SILAC labeling to a relative isotope abundance (RIA) = 1, cells were "chased" with unlabeled media over a period of 8 h (Figure 1). At each time point, proteins were resolved by 1D SDS-PAGE, and from each gel slice, proteins were identified using LC-ESI-ion trap mass spectrometry and database searching. Each time a protein was identified, the partition of peptide ion current between stable isotope labeled and unlabeled variants changed according to the rate at which that protein was replaced in the cell. Proteins selected for turnover calculations were required to be identified in at least three time-points with a significant MOWSE score ($p < 0.05$) and individual peptides used for quantification required a significant ion score ($p < 0.05$). In general, multiple arginine-terminating peptides were used for the calculation of RIA at each time-point and a minimum of three time-points (including t_0, RIA = 1) were used to determine the degradation rate for each protein. A total of 2375 (RIA, t) data points were used to define the degradation rate of 576 nonredundant proteins identified that matched these criteria (Supporting Information). Each data-point was composed of at least two individual peptides with the majority of data-points comprising 3−10 individual peptides. In total, 8643 individual peptide ion pairs were quantified. In addition, each peptide was observed in more than one spectral event and often in multiple gel slices. Intrapeptide variability was minimal (Figure 2C) giving increased confidence in our results. The (RIA, t) data were fitted to a single exponential decay curve (Figure 2), allowing the calculation of the rate of loss of label, k_{loss}. The rate of dilution due to cell growth, k_{dil}, was subtracted to give the true degradation rate constant, k_{deg}, for each protein. The derivation of all equations has been described previously.[15] The calculated degradation rates ranged from $2 \times 10^{-5} \pm 9 \times 10^{-07}$ h^{-1} to 5.4 $\pm$ 0.4 h^{-1}, relating to half-lives of many tens of hours to just 6 min. For the 576 nonredundant values, the mean degradation rate was 0.081 h^{-1} and the median degradation rate was 0.034 h^{-1}. The degradation rate constants were not normally distributed (Kolmogorov−Smirnov test, $P < 0.001$), and although the data could be log-transformed to normality, all statistical analyses have been conducted on untransformed data using nonparametric methods. Although these data generate absolute turnover rates, they cannot be extrapolated to other cell types or tissues without a degree of caution[4,5] and are of greatest value in internal analyses of factors that modulate protein stability.

Inherent Characteristics of Proteins That Determine Degradation Rate. A large turnover data set allows exploration of putative structural characteristics that regulate intracellular turnover rate. It has been postulated that molecular weight and charge of the intact protein have an influence on intracellular turnover rate.[18−20] However, such correlations are sometimes made from data describing the behavior of disparate proteins. In addition to differences between average turnover rates in tissues (for example, skeletal muscle proteins turn over on average 10-times more slowly than those of liver), different species also exhibit different absolute protein turnover rates, such that protein turnover is higher in small than in large mammals.[32,33] Thus, absolute turnover rates vary depending on the source of the protein, and do not form a satisfactory basis for comparison of turnover behavior, since the degradative/proteolytic context may differ. A proper examination of structural features that might dictate degradation rate can only easily be achieved if data on degradation rates can be amassed for different proteins derived from the same cell type and under identical conditions. This requirement leads naturally to a proteome based approach, in which temporal isotope labeling can be used to assess how rapidly a protein is being turned over in the cell. Previously, our work in this area has been based on measurement of isotope labeling curves obtained from proteins resolved by gel electrophoresis and analyzed predomi-

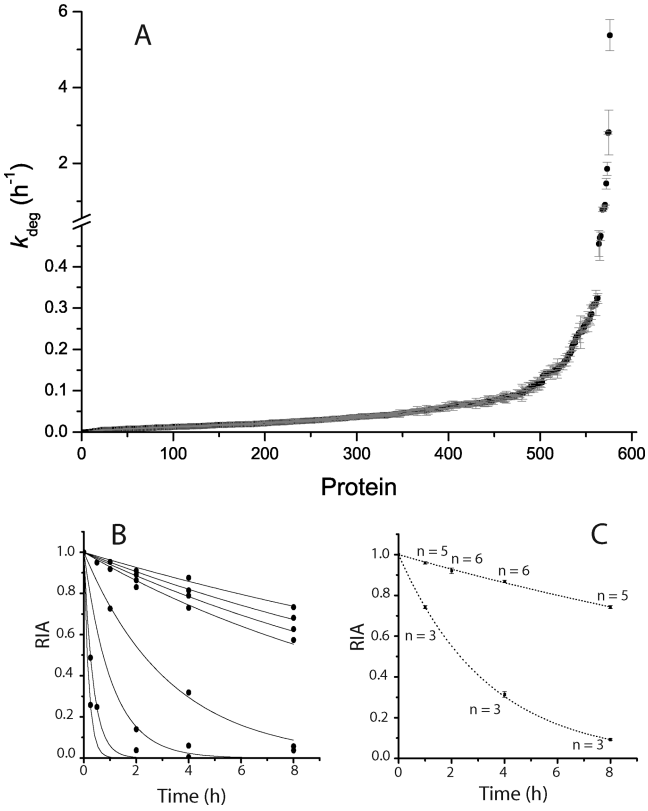

Figure 2. Global analysis of protein degradation. Using the protocol outlined in Figure 1, the change in relative isotope abundance (RIA) for each protein was assessed over the unlabeled 'chase' period. The (RIA, *t*) data were fitted to a single exponential decay curve, yielding the best fit value of the first order rate constant for the degradation of almost 600 unique proteins. The distribution of degradation rate constants is presented in panel A, with exemplar data for the (RIA, *t*) curves, complete with fitted curves (B) and the interpeptide variability (C) shown. In this panel, the degradation plots for two proteins are shown with the spread of data (SD) indicated by the error bars.

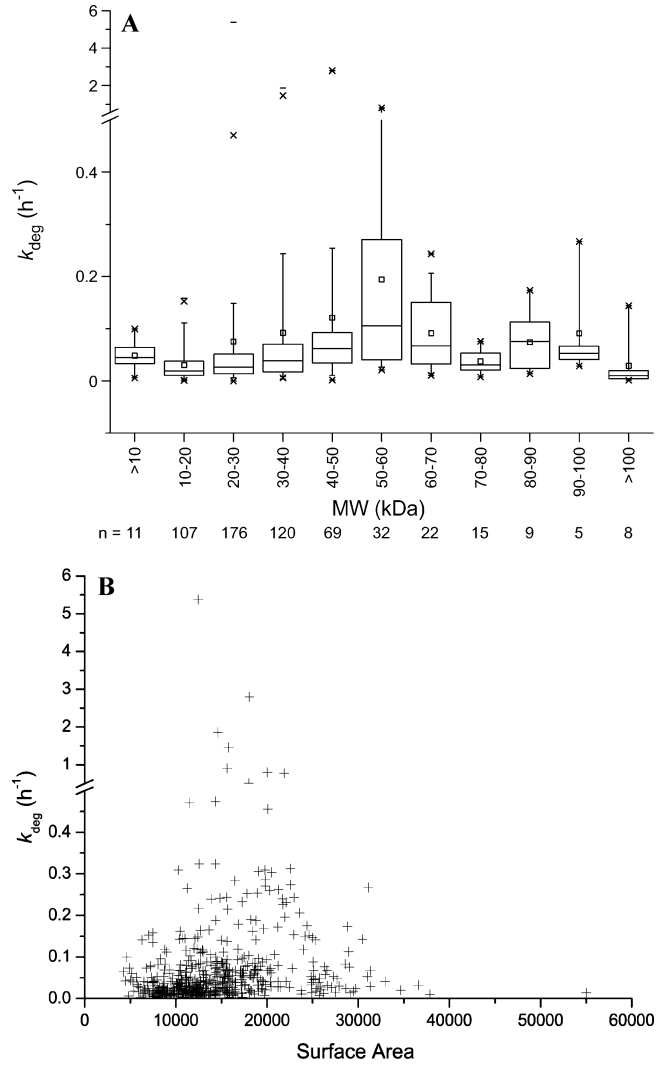

Figure 3. The relationship between protein subunit molecular weight, surface area and rate of degradation. (A) Proteins were grouped in 10 kDa increments from 0 to 100 kDa with all proteins larger than 100 kDa ($n = 8$) grouped into the final category. For each category, the distribution of degradation rate constants is displayed as a box and whiskers plot, reflecting the nonparametric nature of the data set. (B) In a second analysis, the accessible surface area of each protein was calculated and plotted against degradation rate.

nantly by MALDI-ToF mass spectrometry. Although this is effective, it is less well suited to high-throughput determination of degradation rates. To acquire a comprehensive turnover profile, LC-MS based methods are preferred, which is the approach described here. Although this approach yields absolute values for the first-order rate constant for degradation, the collated data are of primary value as an internally consistent, high quality data set that can be used to assess the relationship between relative turnover rate and sequence motifs or physicochemical properties.

Previous work, based on dual isotope radiolabeling of soluble proteins, suggested that high molecular weight proteins tend to be turned over more rapidly than low molecular weight proteins.[18] In addition, a literature search at the time of publication confirmed that this held true for 22 proteins, although even at that time there were examples of small proteins that were rapidly degraded in the cell. To test this hypothesis, we assessed the relationship between degradation rate and the predicted mature molecular weight of the protein subunit. As anticipated, there was a very strong correlation ($r^2 = 0.94$, $P < 0.001$) between predicted molecular weight and mobility on the gel, and it is reasonable to assume that the predicted molecular weight data are valid and useable.

There was no correlation between k_{deg} and molecular weight (slope < 0.0001, $r^2 \sim 0$, $P = 0.31$), but the scatter of the data limits the value of this analysis. Proteins were therefore grouped into molecular weight 'bins' of 10 kDa (Figure 3A), and analyzed nonparametrically, which indicated that the different classes could have been derived from different turnover populations (Kruskal−Wallis test, chi-squared = 102.5, 10DF, $P < 0.001$). Closer inspection of the data distribution indicated that the two extreme categories (<10 kDa and >100 kDa), both 'open' categories, contained relatively few data points. Accessible surface area may be a more relevant parameter than molecular weight to investigate in relation to degradation rate. It could be argued that surface area provides an indication of the extent to which a protein is exposed to external "degradative factors" such as proteases and modifications, including ubiquitination, which signal a protein for degradation. In Figure 3B, degradation rate is plotted against monomer surface area.[34] There

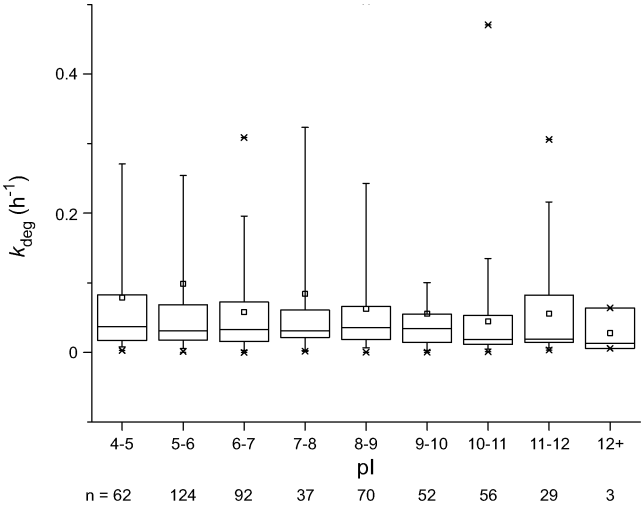

Figure 4. The effect of protein charge on intracellular stability. All proteins in the data set were binned in intervals of 1 pH unit according to the calculated p*I* of the mature protein, and the distribution of degradation rate constants was plotted.

appears to be a bell shaped distribution with an apex at 10 000−20 000 Å^2, although this is not statistically significant. Therefore, our more global study of protein degradation rates does not support a direct relationship between molecular weight and, by corollary, surface area and intracellular stability. There is no satisfactory mechanistic explanation for the behavior, but it warrants further examination.

Dice and Goldberg performed an analogous study to the molecular weight correlation experiment and found a general trend: acidic proteins are less stable than neutral or basic proteins,[19,20] although once again, in their analysis, there were notable exceptions. For example, proteins with an isoelectric point of ∼6 ranged in half-life from 20 min to 60 h. One of the primary restrictions of such analyses is that they focus on averaged "total protein" data and do not look at the degradation rates of individual proteins. Because we determine the intracellular stability of multiple individual proteins, it was possible to implement a more robust analysis, based on the data set resolved into p*I* groups of 1 pH unit. The distribution of k_{deg} values does not change with p*I* (Kruskal−Wallis test, chi-squared = 8.7, 8DF, $P = 0.37$, Figure 4), although it should be noted that the p*I* has been calculated on primary sequence alone and does not take into account any secondary or tertiary effects of protein folding, or any moderation of p*I* by post-translational modification. Finally, proteins were grouped according to their gene ontology (GO) classifications: location, function, process and class. Proteins were classified into 24 locations with the cytoplasm (190 proteins) and the nucleus (106 proteins) dominating. Over 65 different functions were attributed to the proteins along with 25 biological processes. GO "class" stratification resulted in 72 different groupings, falling to 46 when all enzymes (105 proteins) were grouped together. The distribution of rates was determined as a function of each classification. No one GO class exhibited turnover characteristics that differed from another (data not shown).

Correlation of Degradation with Sequence Motif and N-Terminal Amino Acid. One of the most cited determinants of protein stability is the N-terminal amino acid of the mature protein. This is embodied in the N-end rule, as first defined by Varshavsky and colleagues.[26,35,36] Each amino acid is classified as either stabilizing (M, S, A, P, T, G, V) or destabilizing. Destabilizing residues are further segregated into those which require no further processing (primary: R, K, H F, L, W, I, Y); those which must be conjugated to an arginine residue before recognition (secondary: D, E, C) and finally, amide residues which must be hydrolyzed to their corresponding acid form prior to coupling with an arginine residue (tertiary: N, Q). As our protocol relied on in-gel tryptic digestion of proteins, it was rare for the true N-terminal peptide to be identified. Therefore, to determine any correlation between stability and the identity of the N-terminal amino acid, it was necessary to predict the true N-terminus. All protein sequences were analyzed for the presence of predicted signal sequence peptides, and if present, these were removed from the sequence. For proteins expressed without signal peptides, the main processing step is removal of Met_1 by methionine aminopeptidases. These enzymes are thought to excise Met_1 when the second amino acid is one of C, G, A, S, T, V and P.[37] By application of the N-terminal processing rules, it was possible to cluster proteins in those with predicted stabilizing ($n = 499$) and destabilizing ($n = 43$) N-terminal residues (Figure 5A). We therefore tested the hypothesis that the degradation rate of proteins with a destabilizing N-terminal amino acid was different to that of those with stabilizing N-terminal amino acids. Although this yielded a statistically significant result (Mann−Whitney U test, $z = 2.39$, $P = 0.017$), the data implied that proteins bearing N-terminal *stabilizing* residues were degraded more rapidly, contrary to the prediction of the N-end rule. However, it must be recognized that these data are subject to the veracity of the predicted N-terminus.

A further proposed signal for degradation is the presence of PEST sequences within the mature protein. PEST motifs are segments rich in proline (P), glutamic acid (D), aspartic acid (E) and serine (S) or threonine (T) residues. PEST sequences were first proposed as a degradative signal in 1986[23] following a survey of the sequences of proteins known to be rapidly degraded *in vivo*. A total of 45 proteins were analyzed and it was proposed that the presence of this sequence may increase the acidity of proteins or that phosphorylation of amino acids in the sequence may promote calcium mediated proteolysis. More recent analyses[25] indicated that, while the presence of a PEST sequence could not be directly correlated with an elevated rate of degradation in a global analysis, it was more probable to find a PEST sequence in a group of proteins with short half-lives. Each protein sequence was screened using the epestfind program (http://www.at.embnet.org/embnet/tools/bio/PEST-find/) for PEST sequences and the degradation data were grouped according to the presence of a potential or poor PEST sequence or the absence of any motif (Figure 5B). The majority of proteins ($n = 493$) had poor or no PEST sequence motifs with 79 proteins being flagged as containing recognizable PEST motifs. Comparison of these two data groups (potential PEST vs poor/no PEST sequence) indicated that there was no evidence for the hypothesis that rapidly degrading proteins contained PEST motifs (Mann−Whitney U test, $z = -0.87$, $P = 0.39$). However, a comparison between each group indicated that there was a significant difference, such that those proteins with no discernible PEST sequences were degraded more slowly than the other two categories (Kruskal−Wallis test, chi-squared = 7.0, 2DF, $P = 0.03$). However, the largest data group was that where there was weak evidence for PEST sequence, and it is

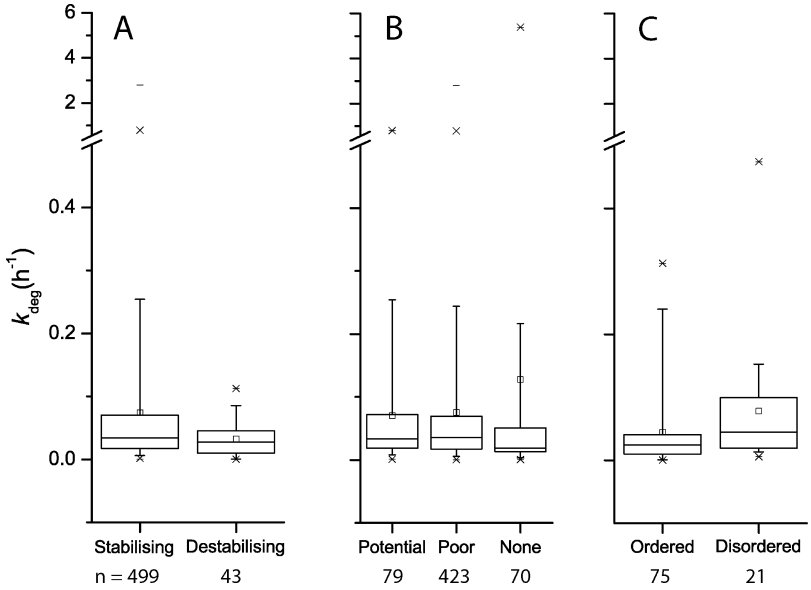

Figure 5. primary sequence and protein stability: proteins were grouped according to the N-end rule hierarchy (A). There was no observed (de)stabilizing effect related to N-terminal amino acid. The sequence of each protein in the data set was analyzed for the presence of PEST sequences and grouped as to whether they contained potential, poor or no PEST sequences (B). The predicted degree of order and disorder was obtained using the primary sequence of each protein. Proteins which were predicted to display zero disorder were compared to those with a 100% disordered structure (C).

difficult to assess the extent to which a lack of a PEST sequence reflects a mechanistic resistance to degradation.

Protein Order as a Primary Determinant of Intracellular Stability. A recent study of the yeast proteome indicated that the strongest, albeit weak, discriminator of protein stability was the inherent degree of disorder dictated by the primary sequence of a protein.[25] While the significance of the correlation between protein stability and the extent of structural disorder was low, it was the only intrinsic property of a protein that invoked any correlation at all. For our data set, obtained from untagged proteins in metabolically viable cells, both the number of long disordered regions (where 'long' means greater than thirty amino acids) and the ratio of disordered amino acids to total amino acids in each protein were compared to its rate of degradation. The number of long disordered regions showed no discrimination between stable and rapidly degraded proteins (data not shown); however, when proteins were classified as those having no disordered residues ($n = 75$) and those which have a completely disordered structure ($n = 21$), the general behavior was to more disordered proteins exhibiting elevated rates of degradation (Figure 5C; Mann−Whitney U test, $z = -2.1$, $P = 0.04$). These data indicate that, although protein disorder may not be the sole determinant of protein stability, it may have a role to play along with other, yet to be defined, biochemical, structural and functional properties of a protein. Indeed, the driver of protein degradation may not be the individual protein alone, but how it interacts with other cellular components, and this may change under different cellular conditions.

Multiprotein Complex Assembly. Although many proteomics studies focus on individual proteins, it is well-recognized that the true proteome is a hierarchical assembly of supramolecular complexes and it will ultimately become necessary to consider proteins in quaternary space—their assembly, partition and dissociation. Proteins can function as cores, modules and attachments[38] recognized from the variance in stoichiometry and in the dynamics of protein exchange. For most of these complexes, it is not known whether the components are turned over as a unit, and if so, by what mechanism, or if some form of disassembly is required prior to the turnover of individual subunits. Moreover, it is not clear whether individual subunits exchange between the free and assembled forms, and whether there are pools (of high or low turnover) subunits in a state of rapid exchange. One parameter that might yield additional information is the relative rate of turnover of individual subunits of complexes. Although not the purpose of the study, for two such complexes (the ribosome and the 20S proteasome), we fortuitously recovered data for a substantial number of subunits, and were thus able to record the turnover dynamics of individual proteins from each complex.

The ribosome comprises an 80S functional particle that repeatedly dissociates into 40S and 60S subunits and then reassembles during translation.[39] Individual ribosomal proteins are expressed at concentrations in excess of the amount required for ribosome-subunit production and there is continuous degradation of unassembled ribosomal proteins in the nucleoplasm, allowing mammalian cells to control the number and synthesis of entire ribosomes. This 'surplus parts' mechanism ensures that protein availability is never rate limiting for the efficient assembly of ribosome subunits.[40,41] The assembly of bacterial ribosomes is sequential and highly regulated.[42] Eukaryotic ribosome assembly, also sequential, is known to involve at least 300 accessory proteins.[43−45] Although the dynamics of the intact 40S and 60S subunits have been examined,[45,46] there is no data describing the degradation rate of the individual subunits.

We identified 27 individual subunits from each of the 40S and 60S ribosome and have measured the degradation rate of each (Figure 6). It is evident that the subunits do not turn over at a uniform rate. In the 40S ribosome, the S15a subunit was most stable with a k_{deg} of 0.0009 h^{-1} (half-life = 805 h), whereas the S6 subunit has a k_{deg} of 0.11 h^{-1} (half-life = 6 h), two orders of magnitude difference in stability. Similarly, the degradation rates of the 60S ribosome range from 0.0048 h^{-1} (L23a, half-

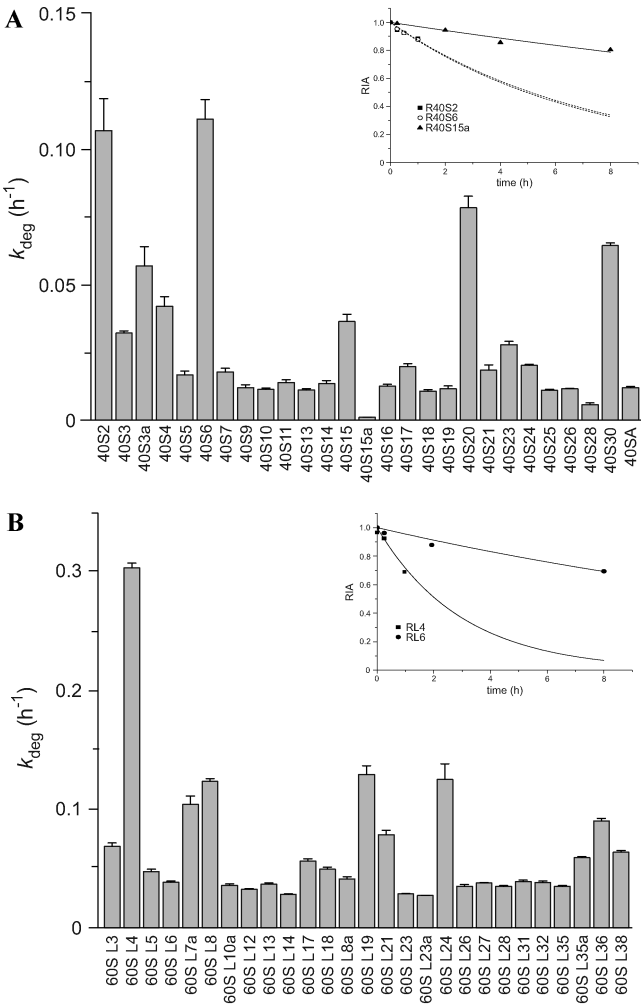

Figure 6. Relative turnover of individual ribosome subunits. The data set were scrutinized for ribosomal subunit proteins, and degradation data for 54 ribosomal subunits were recovered from 40S (A) and the 60S (B) ribosomal subunits. The inset figures show the first-order decay curves for the protein subunits with the highest and lowest rates of degradation.

life = 144 h) to 0.031 h^{-1} (L4, half-life = 2.6 h). The 20S proteasome is a cylindrical structure composed of 28 subunits—α subunits arranged in two heptameric rings flanking two central β subunit seven-membered rings. Although much is known about the assembly pathway of the 20S proteasome,[47−52] it is not clear whether the proteasome is degraded as a single unit or if the individual subunits are capable of reuse. In chicken skeletal muscle, the subunits were synthesized at different rates, and high turnover subunits were featured in both the α (nonproteolytic) and β (proteolytic) rings.[53] In this study, 12 individual subunits were characterized; 6 α and 6 β subunits (Figure 7). Degradation rates ranged from 0.002 h^{-1} (alpha-5; half-life 264 h) to 0.024 h^{-1} (alpha-2; half-life 27 h) and from 0.0002 h^{-1} (beta-1; half-life 3150 h) to 0.0218 (beta-5; half-life 31 h). Interestingly, the 20S proteasome subunits are inherently more stable than the ribosomal subunits. The number of ribosomes directly influence total translational activity in the cell, while the 20S proteasome activity is strongly regulated by the 19S cap structure and substrate delivery mechanisms such as ubiquitination, and it may be that the 20S core of the proteasome has evolved to be a relatively stable entity in the cell.

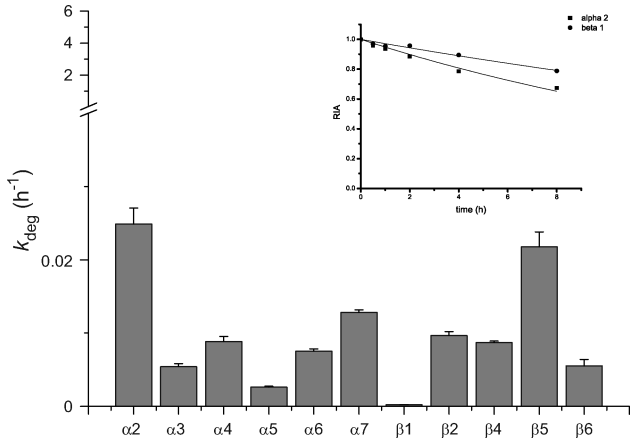

Figure 7. Relative turnover of subunits of the 20S proteasome. The data set were scrutinized for 20S subunit sequences, and turnover data for 12 subunits, six each from the α- and β-rings were recovered.

For both these complex machines, individual protein subunits differ in their intracellular stability. In the absence of information on the state of the proteins (free or assembled), it is dangerous to overinterpret these data, although they imply that some subunits might be reused (core proteins?), while others exchange with assembled ribosomes (attachments?). Further exploration of subunit turnover, especially partitioned between free and assembled subunits might play a key role in defining the dynamics of machine assembly in the cell. It is tempting to speculate that, for both complexes, subunits are synthesized in excess and are available for assembly into the core particle when required.

Conclusion

Temporal proteomics not only encompasses changes at the post-translational level, such as cellular localization, phosphorylation or ubiquitination, but also includes intracellular protein stability. A full definition of a proteome should include detailed and accurate knowledge of the rates at which each protein is synthesized and degraded. Most simplistically, the absolute concentration of a protein in the cell [P] is the result of the competition between a zero order synthesis (defined by k_{syn}) and first order (stochastic) degradation, defined by k_{deg}. In principle then, knowledge of any two of these parameters ([P], k_{syn}, or k_{deg}) would allow calculation of the third. We have recently defined a novel approach to large scale absolute quantification of proteins in the cell,[54−56] and as we have seen in this study, dynamic SILAC can yield k_{deg}. This permits calculation of the rate of synthesis (in molecules per cell per unit time) and we conjecture that this is the parameter that should correlate most strongly with transcript abundance data. Definition of the dynamic proteome is now feasible.

Acknowledgment. This work was supported by BBSRC (BB/C507510/1), CRUK and the RCUK (Academic Fellowship to M.K.D.). We are grateful to Jane Hurst for assistance with the statistical analyses, and to Duncan Robertson for mass spectrometry support.

Supporting Information Available: Table of degradation rates for HeLa proteins identified by LC-MS/MS. This material is available free of charge via the Internet at http://pubs.acs.org.

References

(1) Doherty, M. K.; Beynon, R. J. Protein turnover on the scale of the proteome. *Expert Rev. Proteomics* **2006**, *3* (1), 97–110.
(2) Eagle, H.; Piez, K. A.; Fleischman, R.; Oyama, V. I. Protein turnover in mammaliar cell cultures. *J. Biol. Chem.* **1959**, *234* (3), 592–7.
(3) Ohsumi, Y. Protein turnover. *IUBMB Life* **2006**, *58* (5−6), 363–9.
(4) Millward, D. J. Protein turnover in skeletal muscle. I. The measurement of rates of synthesis and catabolism of skeletal muscle protein using (14C)Na2CO3 to label protein. *Clin. Sci.* **1970**, *39* (5), 577–90.
(5) Millward, D. J. A simple method for measuring protein turnover in the liver: the effects of starvation and low protein feeding on liver protein metabolism in the rat. *Gut* **1971**, *12* (6), 495.
(6) Garlick, P. J.; Millward, D. J. An appraisal of techniques for the determination of protein turnover in vivo. *Biochem. J.* **1972**, *129* (2), 1P.
(7) Waterlow, J. C. Whole-body protein turnover in humans--past, present, and future. *Annu. Rev. Nutr.* **1995**, *15*, 57–92.
(8) Hara, H.; Shiota, H. Differential increases in syntheses of newly identified trypsinogen 2 isoforms by dietary protein in rat pancreas. *Exp. Biol. Med.* **2004**, *229* (8), 772–80.
(9) Choi, K. L.; Wang, Y.; Tse, C. A.; Lam, K. S.; Cooper, G. J.; Xu, A. Proteomic analysis of adipocyte differentiation: Evidence that alpha2 macroglobulin is involved in the adipose conversion of 3T3 L1 preadipocytes. *Proteomics* **2004**, *4* (6), 1840–8.
(10) Hermansson, M.; Sawaji, Y.; Bolton, M.; Alexander, S.; Wallace, A.; Begum, S.; Wait, R.; Saklatvala, J. Proteomic analysis of articular cartilage shows increased type II collagen synthesis in osteoarthritis and expression of inhibin betaA (activin A), a regulatory molecule for chondrocytes. *J. Biol. Chem.* **2004**, *279* (42), 43514–21.
(11) Iresjo, B. M.; Svanberg, E.; Lundholm, K. Reevaluation of amino acid stimulation of protein synthesis in murine- and human-derived skeletal muscle cells assessed by independent techniques. *Am. J. Physiol. Endocrinol. Metab.* **2005**, *288* (5), E1028–37.
(12) Andersen, J. S.; Lam, Y. W.; Leung, A. K.; Ong, S. E.; Lyon, C. E.; Lamond, A. I.; Mann, M. Nucleolar proteome dynamics. *Nature* **2005**, *433* (7021), 77–83.
(13) Cargile, B. J.; Bundy, J. L.; Grunden, A. M.; Stephenson, J. L., Jr. Synthesis/degradation ratio mass spectrometry for measuring relative dynamic protein turnover. *Anal. Chem.* **2004**, *76* (1), 86–97.
(14) Doherty, M. K.; Whitehead, C.; McCormack, H.; Gaskell, S. J.; Beynon, R. J. Proteome dynamics in complex organisms: using stable isotopes to monitor individual protein turnover rates. *Proteomics* **2005**, *5* (2), 522–33.
(15) Pratt, J. M.; Petty, J.; Riba-Garcia, I.; Robertson, D. H.; Gaskell, S. J.; Oliver, S. G.; Beynon, R. J. Dynamics of protein turnover, a missing dimension in proteomics. *Mol. Cell. Proteomics* **2002**, *1* (8), 579–91.
(16) Rao, P. K.; Roxas, B. A. P.; Li, Q. Determination of global protein turnover in stressed Mycobacterium cells using hybrid-linear ion trap-Fourier transform mass spectrometry. *Anal. Chem.* **2008**, *80* (2), 396–406.
(17) Lampert, F. M.; Matt, P.; Grapow, M.; Lefkovits, I.; Zerkowski, H. R.; Grussenmeyer, T. "Turnover proteome" of human atrial trabeculae. *J. Proteome Res.* **2007**, *6* (11), 4458–68.
(18) Dice, J. F.; Goldberg, A. L. A statistical analysis of the relationship between degradative rates and molecular weights of proteins. *Arch. Biochem. Biophys.* **1975**, *170* (1), 213–9.
(19) Dice, J. F.; Goldberg, A. L. Relationship between in vivo degradative rates and isoelectric points of proteins. *Proc. Natl. Acad. Sci. U.S.A.* **1975**, *72* (10), 3893–7.
(20) Dice, J. F.; Hess, E. J.; Goldberg, A. L. Studies on the relationship between the degradative rates of proteins in vivo and their isoelectric points. *Biochem. J.* **1979**, *178* (2), 305–12.
(21) Goldberg, A. L.; St John, A. C. Intracellular protein degradation in mammalian and bacterial cells: Part 2. *Annu. Rev. Biochem.* **1976**, *45*, 747–803.
(22) Bachmair, A.; Finley, D.; Varshavsky, A. In vivo half-life of a protein is a function of its amino-terminal residue. *Science* **1986**, *234* (4773), 179–86.
(23) Rogers, S.; Wells, R.; Rechsteiner, M. Amino acid sequences common to rapidly degraded proteins: the PEST hypothesis. *Science* **1986**, *234* (4774), 364–8.
(24) Belle, A.; Tanay, A.; Bitincka, L.; Shamir, R.; O'Shea, E. K. Quantification of protein half-lives in the budding yeast proteome. *Proc. Natl. Acad. Sci. U.S.A.* **2006**, *103* (35), 13004–9.
(25) Tompa, P.; Prilusky, J.; Silman, I.; Sussman, J. L. Structural disorder serves as a weak signal for intracellular protein degradation. *Proteins* **2008**, *71* (2), 903–9.
(26) Varshavsky, A.; Bachmair, A.; Finley, D. The N-end rule of selective protein turnover: mechanistic aspects and functional implications. *Biochem. Soc. Trans.* **1987**, *15* (5), 815–6.
(27) Chau, V.; Tobias, J. W.; Bachmair, A.; Marriott, D.; Ecker, D. J.; Gonda, D. K.; Varshavsky, A. A multiubiquitin chain is confined to specific lysine in a targeted short-lived protein. *Science* **1989**, *243* (4898), 1576–83.
(28) Johnson, E. S.; Bartel, B.; Seufert, W.; Varshavsky, A. Ubiquitin as a degradation signal. *EMBO J.* **1992**, *11* (2), 497–505.
(29) McLean, L.; Young, I. S.; Doherty, M. K.; Robertson, D. H.; Cossins, A. R.; Gracey, A. Y.; Beynon, R. J.; Whitfield, P. D. Global cooling: cold acclimation and the expression of soluble proteins in carp skeletal muscle. *Proteomics* **2007**, *7* (15), 2667–81.
(30) Schulze, W. X.; Mann, M. A novel proteomic screen for peptide-protein interactions. *J. Biol. Chem.* **2004**, *279* (11), 10756–64.
(31) Prilusky, J.; Felder, C. E.; Zeev-Ben-Mordehai, T.; Rydberg, E. H.; Man, O.; Beckmann, J. S.; Silman, I.; Sussman, J. L. FoldIndex: a simple tool to predict whether a given protein sequence is intrinsically unfolded. *Bioinformatics* **2005**, *21* (16), 3435–8.
(32) Nagy, K. A.; Girard, I. A.; Brown, T. K. Energetics of free-ranging mammals, reptiles, and birds. *Annu Rev Nutr* **1999**, *19*, 247–77.
(33) Jurgens, K. D. Etruscan shrew muscle: the consequences of being small. *J. Exp. Biol.* **2002**, *205* (Pt 15), 2161–6.
(34) Miller, S.; Lesk, A. M.; Janin, J.; Chothia, C. The accessible surface area and stability of oligomeric proteins. *Nature* **1987**, *328* (6133), 834–6.
(35) Varshavsky, A. The N-end rule. *Cell* **1992**, *69* (5), 725–35.
(36) Varshavsky, A. Regulated protein degradation. *Trends Biochem. Sci.* **2005**, *30* (6), 283–6.
(37) Hu, R.-G.; Brower, C. S.; Wang, H.; Davydov, I. V.; Sheng, J.; Zhou, J.; Kwon, Y. T.; Varshavsky, A. Arginyltransferase, its specificity, putative substrates, bidirectional promoter, and splicing-derived isoforms. *J. Biol. Chem.* **2006**, *281* (43), 32559–32573.
(38) Pang, C. N.; Krycer, J. R.; Lek, A.; Wilkins, M. R. Are protein complexes made of cores, modules and attachments? *Proteomics* **2008**, *8* (3), 425–34.
(39) Zemp, I.; Kutay, U. Nuclear export and cytoplasmic maturation of ribosomal subunits. *FEBS Lett.* **2007**, *581* (15), 2783–93.
(40) Lam, Y. W.; Lamond, A. I.; Mann, M.; Andersen, J. S. Analysis of nucleolar protein dynamics reveals the nuclear degradation of ribosomal proteins. *Curr. Biol.* **2007**, *17* (9), 749–60.
(41) Perry, R. P. Balanced production of ribosomal proteins. *Gene* **2007**, *401* (1−2), 1–3.
(42) Williamson, J. R. Assembly of the 30S ribosomal subunit. *Q. Rev. Biophys.* **2005**, *38* (4), 397–403.
(43) Fromont-Racine, M.; Senger, B.; Saveanu, C.; Fasiolo, F. Ribosome assembly in eukaryotes. *Gene* **2003**, *313*, 17–42.
(44) Henras, A. K.; Soudet, J.; Gerus, M.; Lebaron, S.; Caizergues-Ferrer, M.; Mougin, A.; Henry, Y. The post-transcriptional steps of eukaryotic ribosome biogenesis. *Cell. Mol. Life Sci.* **2008**, *65* (15), 2334–59.
(45) Lebreton, A.; Rousselle, J. C.; Lenormand, P.; Namane, A.; Jacquier, A.; Fromont-Racine, M.; Saveanu, C. 60S ribosomal subunit assembly dynamics defined by semi-quantitative mass spectrometry of purified complexes. *Nucleic Acids Res.* **2008**, *36* (15), 4988–99.
(46) Zhao, Y.; Sohn, J. H.; Warner, J. R. Autoregulation in the biosynthesis of ribosomes. *Mol. Cell. Biol.* **2003**, *23* (2), 699–707.
(47) Chondrogianni, N.; Tzavelas, C.; Pemberton, A. J.; Nezis, I. P.; Rivett, A. J.; Gonos, E. S. Overexpression of proteasome beta5 assembled subunit increases the amount of proteasome and confers ameliorated response to oxidative stress and higher survival rates. *J. Biol. Chem.* **2005**, *280* (12), 11840–50.
(48) Fricke, B.; Heink, S.; Steffen, J.; Kloetzel, P. M.; Kruger, E. The proteasome maturation protein POMP facilitates major steps of 20S proteasome formation at the endoplasmic reticulum. *EMBO Rep.* **2007**, *8* (12), 1170–5.
(49) Gerards, W. L.; de Jong, W. W.; Boelens, W.; Bloemendal, H. Structure and assembly of the 20S proteasome. *Cell. Mol. Life Sci.* **1998**, *54* (3), 253–62.
(50) Hirano, Y.; Kaneko, T.; Okamoto, K.; Bai, M.; Yashiroda, H.; Furuyama, K.; Kato, K.; Tanaka, K.; Murata, S. Dissecting beta-ring assembly pathway of the mammalian 20S proteasome. *EMBO J.* **2008**, *27* (16), 2204–13.
(51) Isono, E.; Nishihara, K.; Saeki, Y.; Yashiroda, H.; Kamata, N.; Ge, L.; Ueda, T.; Kikuchi, Y.; Tanaka, K.; Nakano, A.; Toh-e, A. The assembly pathway of the 19S regulatory particle of the yeast 26S proteasome. *Mol. Biol. Cell* **2007**, *18* (2), 569–80.
(52) Kruger, E.; Kloetzel, P. M.; Enenkel, C. 20S proteasome biogenesis. *Biochimie* **2001**, *83* (3−4), 289–93.

(53) Hayter, J. R.; Doherty, M. K.; Whitehead, C.; McCormack, H.; Gaskell, S. J.; Beynon, R. J. The subunit structure and dynamics of the 20S proteasome in chicken skeletal muscle. *Mol. Cell. Proteomics* **2005**, *4* (9), 1370–81.
(54) Beynon, R. J.; Doherty, M. K.; Pratt, J. M.; Gaskell, S. J. Multiplexed absolute quantification in proteomics using artificial QCAT proteins of concatenated signature peptides. *Nat. Methods* **2005**, *2* (8), 587–9.
(55) Pratt, J. M.; Simpson, D. M.; Doherty, M. K.; Rivers, J.; Gaskell, S. J.; Beynon, R. J. Multiplexed absolute quantification for proteomics using concatenated signature peptides encoded by QconCAT genes. *Nat. Protoc.* **2006**, *1* (2), 1029–43.
(56) Rivers, J.; Simpson, D. M.; Robertson, D. H.; Gaskell, S. J.; Beynon, R. J. Absolute multiplexed quantitative analysis of protein expression during muscle development using QconCAT. *Mol. Cell. Proteomics* **2007**, *68*, 1416–27.

PR800641V